

ASM '83 San Francisco



ISBN 0-88986-043-2

**APPLIED SIMULATION
AND MODELLING**

A PUBLICATION OF
THE INTERNATIONAL ASSOCIATION OF SCIENCE AND
TECHNOLOGY FOR DEVELOPMENT — IASTED

ACTA PRESS
ANAHEIM * CALGARY * ZURICH

TABLE OF CONTENTS

	PAGE		PAGE
Hydrodynamic Models for Minimizing Environmental Damage from Coastal Zone Development - D.C. Raney J.N. Youngblood	1	Nuclear Waste Disposal Economics: Modelling the Incentives for Waste Aging - D.G. Dippold P.L. Hoffmann	70
Importance of Mathematical Modelling in Integral Water Treatment Plant Design - S. Vigneswaran N.T. Hung	6	Modelling and Simulation of Railroad Operating Practices: Network Oriented Blocking Problem - A.L. Kornhauser P. Mayewski	75
Simulation of Effects of Groundwater Withdrawal on Consolidation of Layers - A. Das Gupta J. Premchitt	10	Bilinear Balanced Realizations: A Gramian Approach - C.S. Hsu C.A. Crawley U.B. Desai	80
Salinity Propagation in Mobile Bay - J.N. Youngblood D.C. Raney	16	Filtering and Forecasting of Daily Streamflows Using GMDH - H.N. Phien R.B. Cruda	85
An Analysis of the Interaction Between a Submerged Jet and a Receiver-Diffuser in a Reverse Flow Diverter - G.V. Smith R.M. Counce	21	System Modelling of Water Quality by CSMP and DYNAMO for the Hsintien River, Taiwan - L-G. Chen H.N. Phien	89
Development of an Evolution Decision Support System - C.H. Chang	25	Self-Optimizing Simulation Models With Long-Term Goals - R.A. Sheldon	93
Fault Dominance in the Reliability Petri Nets - M.R. Zargham R.G. Reynolds	29	A Microcomputer Based Training System for Simulation Education - G.N. Pitts M.L. Eggen	97
Modelling and Simulation of a Slider Bearing With an Arbitrary Curved Surface - C. Wu	33	Computer Based Engineering Education - S.L. Rice	100
Optimization of Steel Plants Processing Vessels - M. Salcudean R.I.L. Guthrie	36	A New Simplex Procedure for Function Minimization - D.H. Chen Z. Saleem D.W. Grace	104
Dynamic Programming Minimization of Lens Aberrations for Ion Beam Lithography - M. Szilagyi	41	Stokes' Problem With Cross-Flow -- Simple Example of Transient Boundary-Layer Blow-Off - P-C. Lu	108
Influence of Optimum Temperature Operations Policies on Deactivation and Reaction - A. Sadana	45	Simulation of Robot Kinematics During Trajectory Planning - H.W. Townes D.O. Blackketter	113
Comparison of Methods of Flow Computation in Pipe Networks - T. Tingsanchali P.C. Chu	51	Analysis of Transportation Options for Nuclear Waste Management - A Simulation Approach - R.V. Varadarajan R. Gupta	119
A Simulation Model of Prioritized CSMA/CD Protocols - X. Li L.M. Ni	55	A Methodology for the Estimation of Apparent Viscosity in Pulsatile Laminar/Turbulent Tube Flow - S.H.L. Tsang P. Lu	123
Efficient Decentralized State Estimation of Multi Area Power Systems Using Square Root Algorithm - A.K. Mahalanabis G. Ray	60	Reliability Modelling Applied to Plant Equipment Working in Majority Vote Mode - D.M. Barry M.W. Hudson	127
Analysis of System Variables on Irrigation Economics: A Statistical Simulation Approach - J.R. Williams O.H. Buller H.L. Manges	65	The Use of a Generalized Database System for General System Simulation - M.A. Melkanoff Q. Chen	131

	PAGE		PAGE
Waste Heat Exchanger Design: A Case Study in Software Engineering - Z.M. Bzymek P.W. McFadden	136	Working Loss Emissions From Fixed-Roof Storage Tanks - J.R. Beckman	194
Modelling the Choice of Work Schedule: Fixed Hours and Flexitime - P.P. Jovanis A. Moore	140	Multi-Input State Control With Model- Based Offset Elimination - L.D. Durbin	197
Steady State Stability Enhancement Using Static Phase Shifters in Multi-Machine Power Systems - A.M. Sharaf S. Sivakumar	144	Tests of Simulated Reset Observers for Non-Linear Processes - L.D. Durbin	201
Industrial Treatment Plant Model for Wastewaters Containing Nitroglycerin and Nitrated Esters - R.P. Carnahan L. Smith	148	A Probabilistic Model and its Computer Simulation for the Evaluation of Multiprocessor Systems with Preemptive Shared Common Resources - G.H. Franzkowiak R.W. Naro	205
Numerical Studies of a Mathematical Model for Radiolysis of Water - S.K. Dey A. Chatterjee L.L. Magee	151	A Model and its Computer Simulation for the Evaluation of Multiprocessor Systems with Nonpreemptive Shared Common Resources - G.H. Franzkowiak R.W. Naro	211
Optimal Reverse Osmosis System Design - J.D. Jeffers R.P. Carnahan	155		
Simulating Tax Reform Impacts in the Legislative Process - R.H. Downing R.W. Eyerly W. Habcivch D.P. Huegel R.D. Twark	161		
Modelling Emergency Ambulance Systems - M. Heller C. ReVelle J. Cohon	165		
Simulating With an Econometric Model of India: An Analysis of Forecasting Ability and Some Experiments - A.A. Dar	169		
The Use of a Three Parameter Model for the Prediction of Creep Strains - T. Sterrett E. Miller	174		
A Mathematical Model of the Input Characteristics of Laminar Proportional Amplifiers - G.V. Smith	178		
A Model for Calculating the Electrical Stress in HV Stranded 3-Core Cables Using the Charge Simulation Technique - A.Y. Hannalla M.M.A. Salama A.Y. Chikhani	182		
Modelling of Tritium in Rainfall: A Study of United States Cities - J.M. Pise	186		
Digital Simulation of Synchronization of the Wind Turbine Generators Against Power Systems - H.H. Hwang L.H. Man Y.W. Yi	190		

Hydrodynamic Models for Minimizing Environmental Damage from Coastal Zone Development

Donald C. Raney
Professor of Engineering Mechanics
Box 2908
University, Alabama 35486

John N. Youngblood
Professor of Mechanical Engineering
Drawer ME
University, Alabama 35486

INTRODUCTION

Numerical models have great potential for improved environmental impact assessment of development in the coastal zone. In this paper, a two-dimensional depth averaged finite difference hydrodynamic model is used to investigate two examples of construction, or proposed construction, in the coastal zone. The first example is a railroad built on a fill across the flood plains above Mobile Bay, Alabama. The second example is a proposed breakwater and channel relocation at Eastpoint, Florida.

In the Mobile Bay flood plain application, the hydrodynamic model is used to quantify the effect which an existing structure has upon flooding problems which are known to exist along Bayou Sara. The model is applied both with and without the railroad on the flood plains. Changes in flow patterns and flood stage elevation which can be attributed to the railroad are documented.

The fishing fleet at Eastpoint, Florida in Apalachicola Bay desires construction of a rubble breakwater and relocation of the existing Federal Navigation Channel. Apalachicola Bay is one of the most important bays in Florida because of its large freshwater inflow and seafood production. In this case the hydrodynamic model is used to evaluate the potential environmental impact of the proposed project.

THE NUMERICAL MODEL

A two-dimensional depth averaged model (BAY) is used in this investigation. The vertical components of velocity and acceleration are neglected and the general three-dimensional governing hydrodynamic equations are integrated over the water depth. A pseudo three-dimensional effect is present since the equations are forced to satisfy the boundary conditions at the bottom and surface of the water column. A depth-averaged two-dimensional flow field is obtained but three-dimensional geometry can be considered. The most important approximations used in the model are those of constant density and relatively small variations of velocity over the depth, conditions which are reasonably valid much of the time in many estuaries. A rectangular coordinate system is located in the undisturbed water surface.

A major advantage of BAY is the capability of applying a smoothly varying grid to the given study region.¹ This allows efficient simulation of complex geometries by locally increasing grid resolution in critical areas. For each coordinate direction, a piecewise reversible transformation is independently used to map prototype or real space (x,y space) into a computation space (α_1, α_2 space). The transformation takes the form

$$x = a + b\alpha^c$$

where a, b and c are arbitrary constants. By applying a smoothly varying grid transformation which is continuous and which has continuous first derivatives, many stability problems commonly associated with variable grid schemes

are eliminated provided that all derivatives are centered in α space. The transformed basic governing equations of momentum and continuity in α space can be written as

$$\frac{\partial u}{\partial t} + \frac{1}{\mu_1} u \frac{\partial u}{\partial \alpha_1} + \frac{1}{\mu_2} v \frac{\partial u}{\partial \alpha_2} + \frac{g}{\mu_1} \frac{\partial \eta}{\partial \alpha_1} - fv = R_x + L_x$$

$$\frac{\partial v}{\partial t} + \frac{1}{\mu_1} u \frac{\partial v}{\partial \alpha_1} + \frac{1}{\mu_2} v \frac{\partial v}{\partial \alpha_2} + \frac{g}{\mu_2} \frac{\partial \eta}{\partial \alpha_2} + fu = R_y + L_y$$

$$\frac{\partial \eta}{\partial t} + \frac{1}{\mu_1} \frac{\partial}{\partial \alpha_1} [(h+\eta)u] + \frac{1}{\mu_2} \frac{\partial}{\partial \alpha_2} [(h+\eta)v] = 0$$

where

- u = depth-averaged velocity component in the x direction
- t = time
- x,y = rectangular coordinate variables
- v = depth-averaged velocity component in the y direction
- g = acceleration due to gravity
- η = water level displacement with respect to datum elevation
- f = Coriolis parameter
- R_x, R_y = the effect of bottom roughness in x and y directions
- L_x, L_y = the acceleration effect of the wind stress acting on the water surface in the x and y direction
- h = water depth
- $\mu_1, \mu_2 = \frac{\partial x_1}{\partial \alpha_1}, \frac{\partial x_2}{\partial \alpha_2}$

To solve the governing equations, a finite difference approximation of the equations and an alternating direction technique are employed. A space-staggered scheme is used in which velocities, water-level displacement, bottom displacement, and water depth are described at different locations within a grid cell as shown in Figure 1. This solution scheme is similar to that originally proposed by Leendertse.²

Three types of boundaries are involved in the calculations: solid boundaries at fixed coastlines, artificial tidal input boundaries arising from the need to truncate the region of computation and river inflows.

PROBLEM DEFINITION

Mobile Bay Application

Mobile Bay is the terminus of the fourth largest river system, in terms of discharge, in the contiguous United States.³ The river system discharging into Mobile Bay is a complex one as is illustrated in Figure 2. The river system can be considered to start at the confluence of the Alabama and Tombigbee Rivers where the

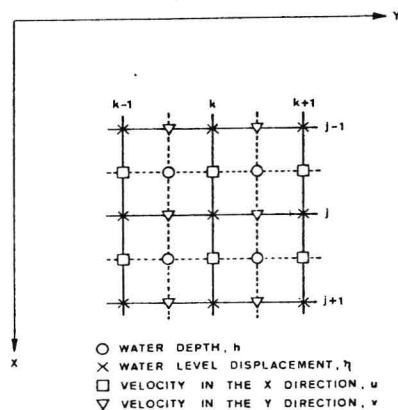


Figure 1. Variable Definition in Finite Difference Cell

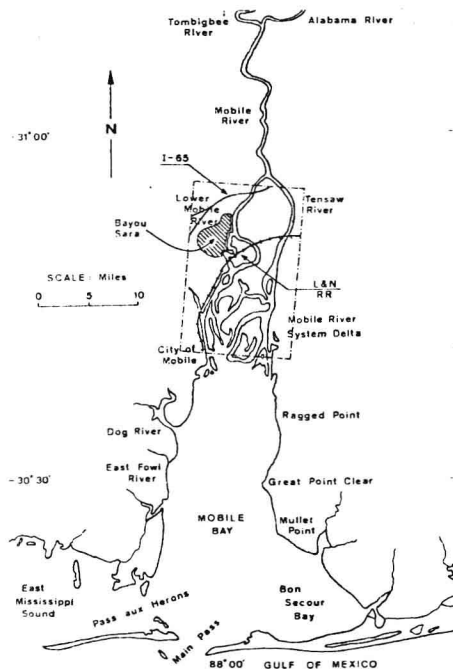


Figure 2. Mobile Bay and Flood Plains

Mobile River is formed. The Mobile River then divides into the Tensaw and lower Mobile Rivers. Both of these rivers branch many times producing a complex network of major channels, creeks, and bayous. The river system flows over a flood plain which extends for over 30 miles south terminating at the northern end of Mobile Bay.

The average discharge of the river system (1929-1978) into the bay is approximately 64,100 cfs.⁴ The monthly average discharges have a high flow in February, March and April and a low flow period between June and November. Significant flooding is considered to occur when flows exceed approximately 247,000 cfs.⁵

A railroad built on a fill crosses the central part of the flood plains. The railroad generally follows a northeast to southwest path across the delta which basically has a north-south alignment. As indicated in Figure 2, Bayou Sara is located in the west-central region of the delta. The geometry of the system suggests that the railroad might have an effect on flood stage elevations along Bayou Sara.

Apalachicola Bay Application

The Apalachicola Bay System, Figure 3, is a barrier island-contained estuary on the Florida Panhandle. The bay system is approximately thirty-nine miles long and an average of six miles wide. There are five flow connections to the Gulf of Mexico; Indian Pass, West Pass, Sikes Cut, St. George Sound and East Pass. All of the openings are natural except Sikes Cut which was originally dredged across St. George Sound in 1954. The primary fresh water flow into the estuary is from the Apalachicola River.

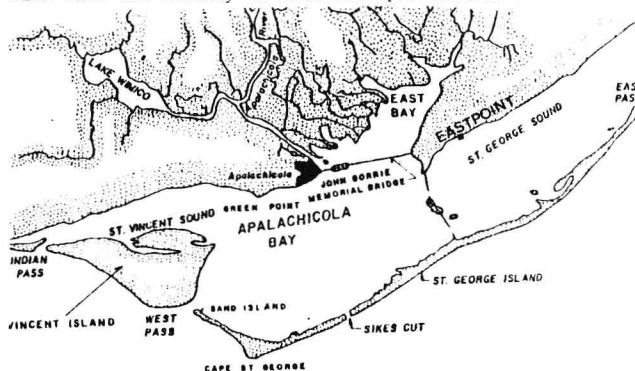


Figure 3. Apalachicola Bay

The bay system is shallow, the mean depth being only about ten feet. The system is generally well mixed with wind effects contributing significantly to circulation patterns. The tides in the area are semi-diurnal with a mean diurnal range of about 1.6 ft.

There is an existing channel generally parallel to shore at Eastpoint. The channel is 6 ft deep, 100 ft wide, and about 6000 ft long with a connecting channel 6 ft deep and 100 ft wide to water of the same depth in St. George Sound. The fishing industry at Eastpoint desires the construction of a breakwater to provide a safe sheltered harbor for the large number of oyster skiffs and small shrimp trawlers operating from the area.

Several different breakwater configurations have been proposed. The breakwater system used in this investigation consists of about 5000 ft of rubble breakwater located 500 ft offshore and generally parallel to the shore. This breakwater was used to establish the general zone of influence of the project rather than investigation of a specific project design.

THE FINITE DIFFERENCE GRID

Mobile Bay Application

The finite difference grid, Figure 4, used to model the Mobile Bay delta system was developed using a 1:24000 scale nautical chart. A variable grid was developed with the primary objective of good resolution of the main river channels and the area around Bayou Sara. The dimension of the resulting grid was 78 by 38 or 2964 cells. A set of aerial photographs⁶ of the delta region taken during February 1982 was also useful in developing the finite difference grid and other input data for the numerical model. Information on construction details of the railroad across the flood plains was also used in establishing the finite difference grid.

The smallest cells were used in representing the area around Bayou Sara since this was the region of primary interest. Small cells were also used for the major river channels. Larger cells were used on the flood plain areas where the bathymetry was reasonably constant and/or boundary geometry was relatively simple. The smallest cell size was 500 ft and the maximum depth was approximately 45 ft.

Elevation boundary conditions were specified at the

LEGEND:
 □ LAND CELL, ▨ FLOOD PLAIN CELL, ■ MAJOR CHANNEL CELL

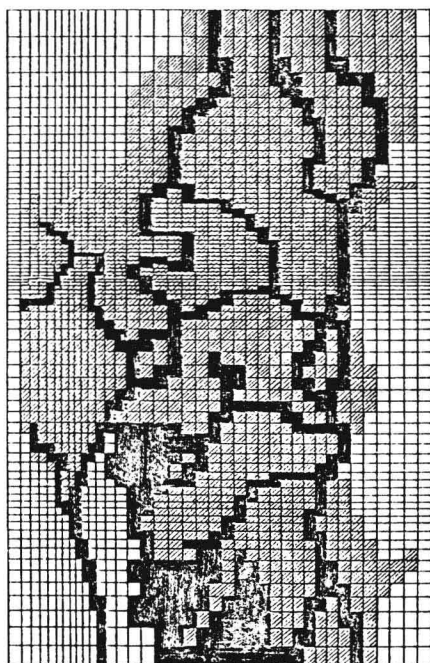


Figure 4. Finite Difference Grid for Mobile Bay Flood Plain Application

Mobile Bay boundary and at the upstream boundary. The Mobile Bay elevation is primarily dominated by the tide while the elevation boundary condition specified at the upstream boundary is representative of the flood stage.

Apalachicola Bay Application

The finite difference grid, Figure 5, used for the model of Apalachicola Bay was developed using a 1:80000 scale nautical chart. A variable grid was developed with the primary objective of good resolution of the proposed breakwater and navigation channel. In addition, good resolution of geometry is desired for all passes opening into Apalachicola Bay. The dimension of the resulting grid was 69 by 42 or 2898 cells.

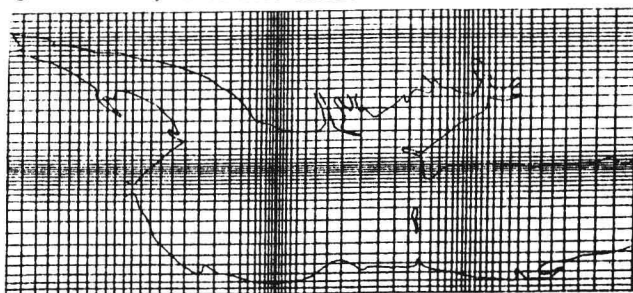


Figure 5. Finite Difference Grid for Apalachicola Bay

The smallest cells were used in representing the area around Eastpoint since this was the region of primary interest. Small cells were also used for the passes. Larger cells were used in areas of the bay where the bathymetry was reasonably constant and/or boundary geometry was relatively simple. The smallest cell size was 500 ft and the maximum depth was approximately 50 ft.

A tidal boundary condition was specified at all passes entering Apalachicola Bay, including Sikes Cut. A constant

river inflow, representing average conditions, was applied simulating the Apalachicola River.

MODEL CALIBRATION AND VERIFICATION

A numerical model must be calibrated and verified before a great deal of confidence is placed in the model results. Calibration consists of demonstrating that the numerical model can be adjusted to produce results which are consistent with a measured prototype data set. Verification consists of applying the calibrated model and reproducing a second set of prototype data to a reasonable degree of accuracy.

Mobile Bay Application

For this study one relatively complete set of prototype data was available representing high water elevations around the delta region for the flood event of March 1979. This data set was used to calibrate the model. A partial data set of high water elevations was available for the April 1979 flood event. These data were used to provide a limited verification of the numerical model.

The measured high water elevations at I-65 (the upper limit of model) provided a basis for establishing the northern elevation boundary conditions for model calibration. The tidal elevations measured in Mobile Bay provided the boundary condition for the southern boundary of the model. Prototype flood stage elevations at 13 locations in the delta region and the system flow rate were the primary variables used in establishing model calibration and verification. The calibration and verification process was continued until agreement was reached between the numerical model and the prototype data sets.

Apalachicola Bay Application

There is very little prototype data for Apalachicola Bay of the quality and synoptic nature required for calibration and verification of numerical models. A limited amount of data are presented in a report by Zeh⁷ and these data are used to provide a partial qualitative calibration of the model. Measured tidal elevations for the Gulf, at a position in Apalachicola Bay near Sikes Cut, and at Apalachicola for August 9, 1978 were available as well as volumetric discharges from Sikes Cut. No velocity data in the interior of the Bay were reported. No specific wind velocity or river flow data were reported for this period. The river flow rate was estimated to have been moderate while the wind was reported as light.

The measured Gulf tide was applied to the numerical model at all openings between the Gulf and the Bay. An average river flow rate of 23500 cfs⁸ was used for Apalachicola River. A no wind condition was used in the model since only a light wind existed when prototype data were taken.

Model parameters were adjusted until the model satisfactorily reproduced the limited amount of prototype data. The limited amount of data available prevented a complete model calibration. It was possible, however, to conclude that the model was producing results qualitatively consistent with the behavior of the physical system. The model should, therefore, be capable of predicting trends which should be produced by changes in the physical characteristics of the system.

MODEL APPLICATIONS AND RESULTS

Mobile Bay Application

Different flood events were considered with a range of flow rates between approximately 200,000 cfs and 800,000 cfs. This range of flow rates contains the 2 year, 5 year, 25 year, 50 year, 100 year and 500 year probability flood events. For each set of boundary conditions there were two model applications. The first model application was for existing conditions; i.e., with the railroad crossing the flood plains. The railroad fill was then replaced by

flood plains with friction and depth characteristics similar to surrounding areas.

Figure 6 illustrates the calculated flood stage elevations as a function of flow rate at one of the 13 special gage points in the delta system where prototype data were available. Results for existing conditions and for the without railroad case are presented in the figure along with prototype data used for calibration and verification. The numerical model was found to be in general agreement with prototype data for the entire delta region.

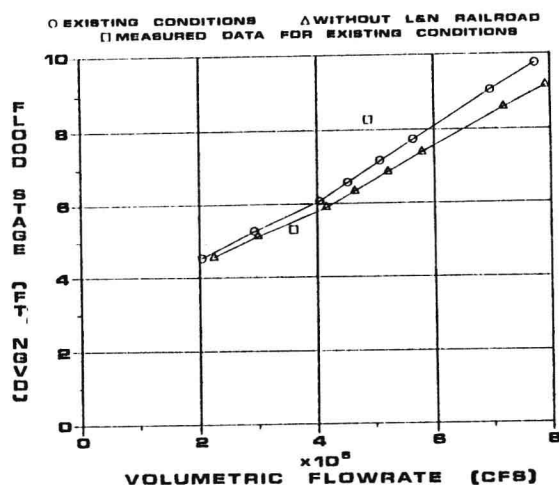


Figure 6. Flood Stage on Bayou Sara as a Function of Flow Rate

Representative contour plots of flood stage elevation in the delta region are presented in Figures 7 and 8. Figure 7 is for the existing condition and Figure 8 is for the case without the railroad on the flood plains. Figure 9 represents a contour plot for the difference in flood stage elevation which can be attributed to the railroad crossing the flood plains.

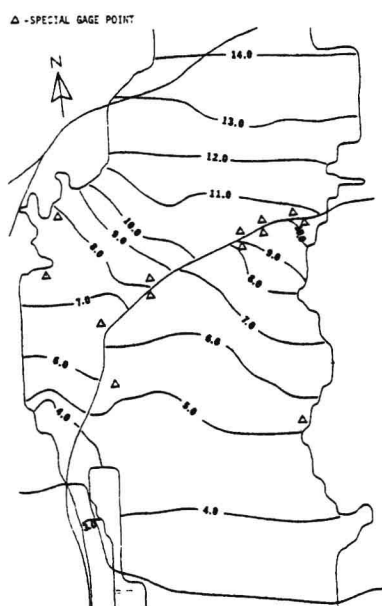


Figure 7. Flood Stage Contours (in feet) in the Mobile Bay Delta Region for a Flow Rate of 558,596 cfs

The velocity patterns produced by the model clearly indicated that most of the flow passes along the existing

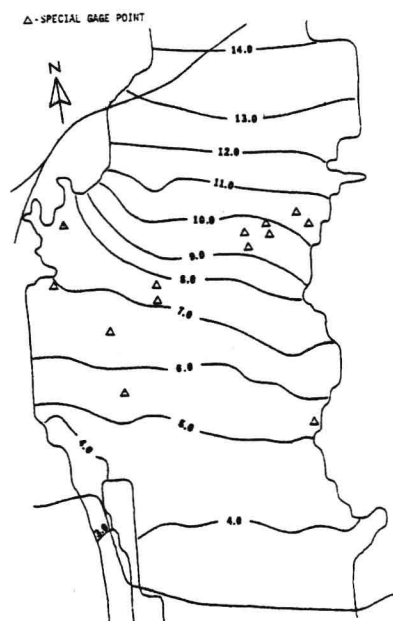


Figure 8. Flood Stage Contours (in feet) in the Mobile Bay Delta Region (without L&N RR) for a Flow Rate of 575,173 cfs

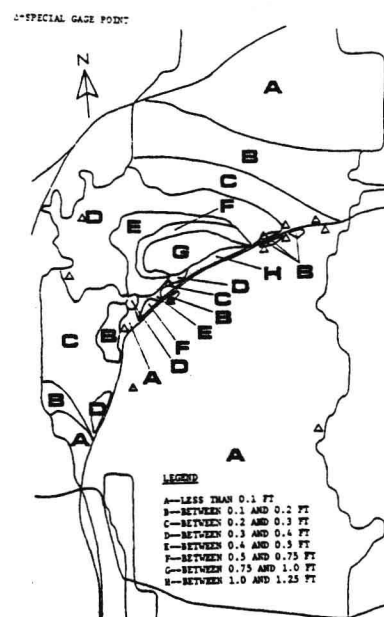


Figure 9. Differences in Flood Stage Elevations in the Mobile Bay Delta Region as a Result of the L&N Railroad for a Flow Rate of Approximately 565,000 cfs

channels regardless of whether the railroad exists or does not exist on the flood plains. There is a great deal of water stored on the flood plains, but there is not a large quantity of flow along (north to south) or across (east to west) the flood plains. The large friction and small depth conditions on the flood plains are not conducive to large flows.

Apalachicola Bay Application

The hydrodynamic model was applied for three basic conditions; no wind, an average summer wind and an average winter wind. The average summer wind was taken as 7.4 mph

at 190° from the north (measured clockwise). The average winter wind was 7.8 mph at 65° from the north. For all runs the same tidal cycle was used, corresponding to the measured tidal cycle of August 9, 1978. An average flow rate of 23,500 cfs was used for the Apalachicola River. In all three cases the model was applied both for existing conditions and with a breakwater installed at Eastpoint. Overall circulation patterns in Apalachicola Bay were compared for the with and without breakwater condition. Circulation patterns in the immediate area of Eastpoint were considered in detail. Figures 10 and 11 indicate a typical circulation pattern in the Eastpoint local area and changes in circulation in the local area which could be expected from the addition of the breakwater.

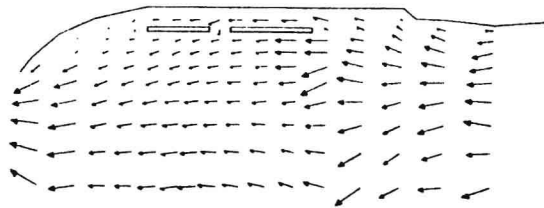


Figure 10. Typical Circulation Pattern in the Eastpoint Local Area

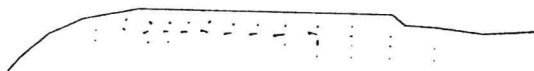


Figure 11. Typical Change in Circulation Pattern Produced by Breakwater at Eastpoint

CONCLUSIONS

Mobile Bay Application

The flows in the delta region are found to be primarily within the existing channels with only a relatively small percentage of the flows along or across the flood plains. Significant differences in flood stage elevations are produced by the railroad within some interior regions of the delta; i.e., across the railroad fill. However, these regions where significant effects are observed are confined to restricted regions within the interior of the delta. The effects are relatively small around the boundaries of the delta.

Based upon the numerical model results, the increase in flood stage elevation along Bayou Sara is small compared with the overall flood stage elevation. Below a system flow rate of 200,000 cfs there is a negligible effect caused by the railroad. On a statistical basis, a 200,000 cfs flow rate corresponds to a flood event which should occur once each year. The railroad effect at Bayou Sara increases up to approximately 6 to 8 inches for a flow rate of 700,000 cfs. A 700,000 cfs flow rate corresponds to a flood event which has a 500 year statistical rate of occurrence. The effects of the railroad on flood stage elevations along Bayou Sara is therefore small compared with overall flood stage elevations.

Apalachicola Bay Application

Based upon numerical model results, the proposed breakwater at Eastpoint should have an almost negligible effect upon overall tidal circulation in Apalachicola Bay for average tide, wind and river flow conditions. Measurable changes in tidal elevation and velocities produced by addition of the Eastpoint breakwater are basically confined to a two mile radius from Eastpoint. Even within

the local Eastpoint area, changes produced by the breakwater are small. Changes in water surface elevation are barely perceptible while maximum changes in velocity around the breakwater are much smaller than 0.1 fps.

No extreme wind, river or tide conditions were considered in this study. No water quality parameters have been directly examined in this study; however, water quality changes can be inferred from the hydrodynamic results. Only local changes in water quality parameters would appear likely.

ACKNOWLEDGMENT

This work is a result of research sponsored in part by NOAA Office of Sea Grant Department of Commerce under Grant #NA81AA-D-00050, the Mississippi-Alabama Sea Grant Consortium, the Mobile District Corps of Engineers and The University of Alabama. The U.S. Government is authorized to reproduce and distribute reprints for government purposes notwithstanding any copyright notation that may appear hereon.

REFERENCES

1. Wanstrath, J.J., Whitaker, R.E., Reid, R.O. and Vastand, A.C., "Storm Surge Simulation in Transformed Coordinates, Vol. I - Theory and Application", Technical Report 76-3, U.S. Army Coastal Engineering Research Center, CE, Fort Belvoir, VA, November, 1976.
2. Leendertse, J.J., "Aspects of Computational Model for Long-Period Water-Wave Propagation", RM-5294-PR, Rand Corporation, Santa Monica, CA, 1967.
3. Morisawa, M., "Streams, Their Dynamics and Morphology", McGraw-Hill, New York, 1968.
4. Schroeder, W.W., Riverine Influence on Estuaries: A Case Study, in M.S. Wiley (ed.), Estuarine Interactions, Academic Press, Inc., New York, 1978, pp.347--364.
5. Bault, E.I., "Hydrology of Alabama Estuarine Areas - Cooperative Gulf of Mexico Estuarine Inventory", Alabama Marine Res. Bulletin 7, pp. 1-36, 1972.
6. Aerial Survey Photographs by Continental Aerial Surveys under contract to U.S. Army Corps of Engineers, Mobile District, February 22-26, 1982.
7. Zeh, T.A., "Sikes Cut-Glossary of Inlet Report No. 7", Report Number 35, Florida Sea Grant College, Department of Coastal and Oceanographic Engineering, University of Florida, August 1980.
8. Personal communications from Dru Barrineau, Planning Division, U.S. Army Corps of Engineers, Mobile District to Dr. Donald C. Raney, Professor, The University of Alabama.

IMPORTANCE OF MATHEMATICAL MODELLING IN INTEGRAL WATER TREATMENT PLANT DESIGN

S. Vigneswaran and N.T. Hung

Asian Institute of Technology, P.O. Box 2754, Bangkok, Thailand

ABSTRACT

This paper presents a methodology for the techno-economical choice of design parameters of a water treatment plant with the help of a limited number of bench-scale experimental results. This approach consists of three main parts:

- The choice of simple mathematical models for each unit operation involved in water treatment and the estimation of empirical coefficients appearing in these models from the bench-scale experimental results for the particular water to be treated.
- The formulation of cost functions for capital and operational and maintenance costs for local conditions.
- The simulation of the technical performance and cost of the whole water treatment plant for different combinations of design parameters and the selection of the optimum design parameters which satisfy the effluent standard at minimum capital and operational and maintenance costs.

INTRODUCTION

Conventional water treatment plants consist of unit operations of flocculation, sedimentation and filtration. The design parameters of these unit operations are generally determined from pilot-scale experiments (with the particular raw water to be treated) or taken directly from the design data of existing treatment plants. But the treatment capacity can be improved considerably in an economical manner by choosing the design criteria for the whole water treatment plant in a rational way.

This paper, therefore, discusses how a techno-economical choice of design parameters can be made using a limited number of laboratory-scale experiments. This methodology requires the mathematical modelling of whole water treatment plant operations.

MATHEMATICAL MODELLING OF INDIVIDUAL UNIT OPERATIONS

Numerous mathematical formulations are available to predict the performance of each of the unit operations involved in a water treatment plant. In this study relatively simple mathematical models are used to formulate the integral water treatment plant model. In each mathematical model, there exists several coefficients which are characteristic of the particular water that needs to be treated and of the types of flocculant and filter media employed. Therefore a limited number of bench-scale experiments using the particular water to be treated is indispensable for calculating these values. In this study an artificial suspension of kaolin clay was used. Cat-floc-T and anthracite (Effective size = 0.92 mm) were used as flocculant and filter media respectively. The mathematical models used are presented below briefly.

1. Flocculation

Boadway's (1978) equation to describe the floc growth is as follows:

$$\ln \frac{d_f}{1 - \frac{d_f}{d_u}} = \ln \frac{d_p}{1 - \frac{d_p}{d_u}} + \alpha_1 t \quad (1)$$

In order to calculate the temporal variation of floc size, the values of ultimate floc size (d_u) and the flocculation coefficient characteristic of the water and operating parameters used (α_1) should be known. Past experience (Boadway, 1978) indicates that α_1 and d_u are functions of velocity gradient and suspended solid concentration for the given flocculant and water to be flocculated. For example for the flocculation of kaolin clay suspension in the presence of Cat-floc-T polymer, the values of α_1 and d_u at different velocity gradients and suspended concentration are given by Liang (1982) as follows:

$$d_u = 219.7 G^{-0.395} C^{-0.013} \quad (2)$$

$$\alpha_1 = 0.053 G^{1.022} C^{-0.657} \quad (3)$$

2. Sedimentation

In the unit operation of sedimentation, the suspended solids removal efficiency (R) was determined (with the assumption that class I settling holds true) using the following equation:

$$R = (1 - C_{v_s}) + \frac{1}{v_s} \int_0^{C_{v_s}} v \cdot d C_v \quad (4)$$

The evaluation of the removal efficiency at a given overflow rate requires an experimental column settling analysis of the flocculated suspension. From the column settling analysis of flocculated kaolin clay suspension, the following semi-empirical relationship was established between the fraction of particles settled (C_v) and the settling velocity (V).

$$C_v = 1.362 V^{0.227} \quad (5)$$

Substituting Eq. (5) in Eq. (4) and solving, one obtains:

$$R = 1 - 1.362 V_s^{0.277} + 0.25 \cdot V_s^{0.23} \quad (6)$$

3. Filtration

As indicated earlier, there are many mathematical formulations available to predict the filter performance. In this study O'Melia's model (1978) was used and is briefly presented below.

The single collector removal efficiency of a filter grain and its associated particles can be calculated from the following equation.

$$\eta_r = \alpha_2 \eta + N \alpha_p \eta_p \left(\frac{d_p}{d_c}\right)^2 \quad (7)$$

The variation of particle collectors (N) with time can be calculated from the following equation.

$$\frac{\partial N}{\partial t} = \beta \cdot n \cdot \alpha_2 \eta \cdot V_o \cdot \frac{\eta}{4} d_c^2 \quad (8)$$

From the material balance of suspended particles removal, the following equation can be written.

$$\frac{\partial n}{\partial t} + V_o \cdot \frac{\partial n}{\partial L} + \frac{3}{2} \frac{(1-f)}{d_c} V_o \cdot n \cdot \eta_r = 0 \quad (9)$$

The effluent concentration (n) can be calculated at different filter depths and filtration times by solving Eqs. (7), (8) and (9). Since there are no analytical solutions available, these equations are solved for n using the forward finite difference method with the following boundary and initial conditions.

$$\eta_r(L, 0) = \alpha_2 \eta \quad (10)$$

$$\eta_r(0, t) = \alpha_2 \eta + a(t - \Delta t) \quad (11)$$

$$\text{where } a = \alpha_p \beta \cdot \eta_p \alpha_2 \cdot V_o \cdot \frac{\eta}{4} d_p^2 \cdot n_o \cdot \Delta t$$

To solve these equations for n, the values of $\alpha_2 \eta$ and $\alpha_p \beta$ should be known. Since these values are characteristic of a particular water, filter media and flocculant used in addition to the operating parameters, a bench-scale experimental study is necessary. The $\alpha_p \beta$ relationship established for the filtration of kaolin clay suspension through anthracite medium is as follows:

$$\alpha_p \beta = 0.035 V_o^{-0.028} C^{-1.134} d_F^{-1.765} \quad (12)$$

The value of $\alpha \eta$ was calculated from clean bed filter experimental results using the Equation:

$$\ln \frac{n}{n_o} = -\frac{3}{2} (1-f) \cdot \alpha \eta \cdot \frac{L}{d_c} \quad (13)$$

The headloss at different filtration times and at different filter depths is calculated from the following equation.

$$\frac{h_f}{\Delta L} = \frac{36k_z \cdot V_o \cdot \mu \cdot (1-f)^2}{d_c^2 \cdot \rho_s \cdot g \cdot f^3} \left[\frac{1 + \beta' \left(\frac{N_p}{N_c}\right) \left(\frac{d_p}{d_c}\right)^2}{1 + \left(\frac{N_p}{N_c}\right) \left(\frac{d_p}{d_c}\right)^3} \right]^2 \quad (14)$$

In the above equations, the number of grains (N_c) at a given depth interval (ΔL) and the number of particles retained (N_p) in j^{th} layer and at i^{th} time step are calculated as:

$$N_c = \frac{\Delta L \cdot A_F \cdot (1-f)}{\eta d_c^3 / 6} \quad (15)$$

$$N_{p_{i,j}} = \sum_{j=1}^{\infty} \sum_{i=1}^{\infty} (n_{1,j} - n_{1,j+1}) \cdot V_o \cdot \Delta T \cdot A_F \quad (16)$$

TECHNICAL PERFORMANCE OF AN INTEGRAL WATER TREATMENT PLANT

Once the coefficients involved in the individual unit operations are estimated for the particular conditions using bench-scale experimental results, the performance of the whole water treatment plant can be evaluated in the

manner sketched in Fig. 1.

An example of the calculation performed is as follows:

- (i) The floc size at different flocculation times for kaolin clay suspension can be calculated using Eqs. (1), (2) and (3) (Fig. 2).
- (ii) The number of flocs can then be calculated by knowing the floc size and the percentage of water in the floc from the following formula.

$$\eta_F = \frac{C_o}{d_F^3 \cdot \rho_s \cdot F_r \cdot \eta / 6} \quad (17)$$

For example, if the kaolin clay suspension of 50 mg/l is to be flocculated to 17 μm , then the number of flocs at the flocculator effluent will be (assuming the floc contains 88% of water) 1.54×10^5 flocs/ml.

- (iii) The removal efficiency in the sedimentation operation for flocculated kaolin clay suspension can be calculated using Eq. (6).

For example at an overflow rate of 2 m/h, the removal efficiency of the flocculated kaolin clay suspension is 59% (from Eq. 6). The removal efficiencies calculated at various overflow rates are presented in Fig. 3.

- (iv) The non-settled flocs in the suspension enter into the filter and the removal efficiency and headloss can be calculated from Eqs. (7) through (16). The headloss development at different filtration rates is presented in Fig. 4.

ECONOMICAL CONSIDERATION OF INTEGRAL WATER TREATMENT PLANT DESIGN

As Dick (1982) pointed out, it is essential to consider the economics of integral water treatment plant design without which this study would be meaningless. In the present study, empirical relationships established between cost and basic design parameters (Table 1) were used to make an economical evaluation.

Table 1 - Cost Functions for Different Operations* (Clark, 1982)

Unit Operations	Cost Functions
1) Flocculation	
a) Capital cost (C_{p1})	$C_{p1} = 212.6 V_F^{0.692} \cdot 1.001^G$
b) O and M cost (C_{mo1})	$C_{mo1} = 11.63 V_F^{0.785} \cdot 1.008^G$
2) Sedimentation	
a) Capital cost (C_{p2})	$C_{p2} = 190.7 A_S^{0.701} \cdot CCI^{0.993} UN$
b) O and M cost (C_{mo2})	$C_{mo2} = 5253 A_S^{0.479} \cdot PPI^{0.178} \cdot DHR^{0.746} \cdot UN^{1.006}$
3) Filtration	
a) Capital cost (C_{p3})	$C_{p3} = 1806.2 A_F^{0.578} \cdot CCI^{0.994}$
b) Backwashing cost	It is calculated on the basis of the cost of the water used for backwashing.

* The calculation of capital and operational and maintenance cost is based on an assumed interest rate of 8% and a design period of 20 years.

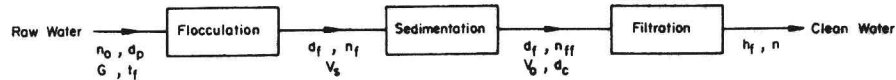


Fig. 1 - Flow Diagram of a Water Treatment Plant

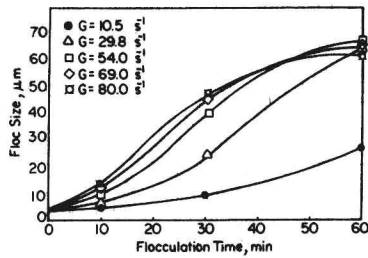


Fig. 2 - The Relationship between d_f, G and t_f ($C_0 = 50 \text{ mg/l}$; $d_f = 5 \mu m$; Dose of Cat-floc T = 0.05 mg/l)

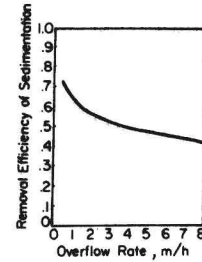


Fig. 3 - The Relationship between Removal Efficiency of Sedimentation and Overflow Rate ($d_f = 0.0017 \text{ cm}$)

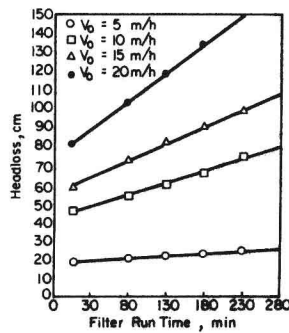


Fig. 4 - The Relationship between Headloss, Filtration Velocity and Filter Run Time ($C_0 = 50 \text{ mg/l}$; $d_f = 5 \mu m$; Dose of Cat-floc T = 0.05 mg/l)

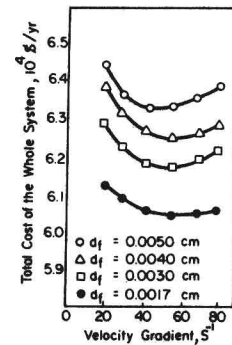


Fig. 5 - Total Cost of the Whole System in Terms of Velocity Gradient ($C_0 = 50 \text{ mg/l}$; $d_f = 5 \mu m$; Dose of Cat-floc T = 0.05 mg/l)

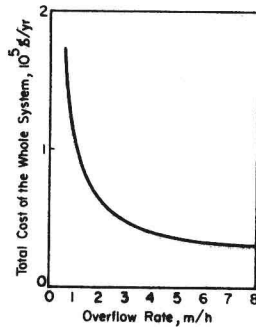


Fig. 6 - Total Cost of the Whole System in Terms of Overflow Rate (Flow = $80,000 \text{ m}^3/\text{d}$; $d_f = 0.0017 \text{ cm}$; $G = 54 \text{ s}^{-1}$; $V_0 = 15 \text{ m/h}$)

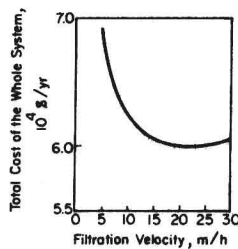


Fig. 7 - Total Cost of the Whole System in Terms of Filtration Velocity (Flow = $80,000 \text{ m}^3/\text{d}$; $d_f = 0.0017 \text{ cm}$; $G = 54 \text{ s}^{-1}$; $V_s = 2 \text{ m/h}$; $d_c = 0.092 \text{ mm}$)

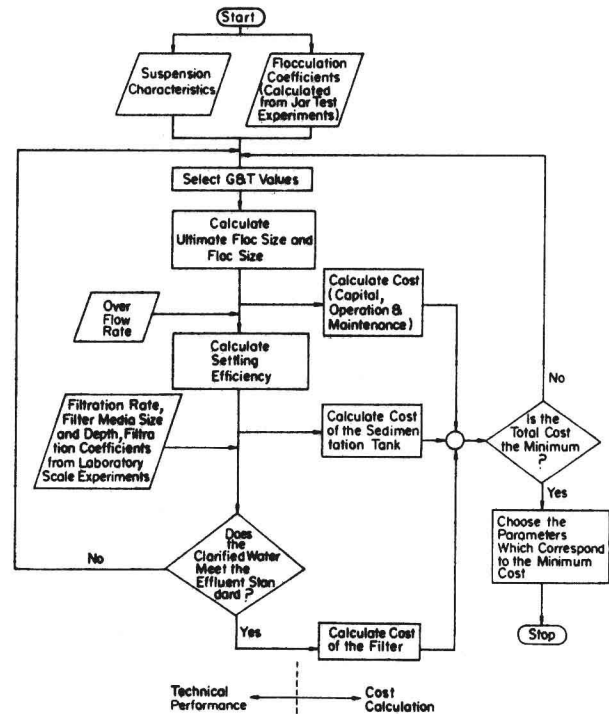


Fig. 8 - Techno - Economical Evaluation of Integral Water Treatment Design

Figs. 5, 6 and 7 present the total cost of the whole system at different flocculation conditions, overflow rates and filtration rates respectively. Once the mathematical formulations for predicting the performance and cost are known, the techno-economical analysis of the whole water treatment plant can be performed in the manner illustrated in Fig. 8.

CONCLUSION

In summary, there are many parameters like G , t_p , V_s , V_o , d_c , L which would affect the performance of a water treatment plant. There can be numerous combinations of these operating parameter values, which would meet the effluent standards. But it is necessary to perform an economic analysis in order to choose the most economical design which involves the least capital, and operational and maintenance cost. The techno-economical approach of this type can be used to design a water treatment plant. However, certain assumptions made during the development of this model limit the direct use of the model in real cases.

NOTATION

A_p	Surface area of retained particles	cm^2	L	Filter depth	cm
A_c	Surface area of clean bed filter media	cm^2	N	Number of particle collectors	No. of particles/ cm^3
A_f	Cross-sectional area of the filter	m^2	N_c	Number of filter grains in a unit length of filter bed	-
A_s	Sedimentation tank area	m^2	N_p	Number of particles retained in a unit length of filter bed	-
C	Suspended solids concentration	NTU	n	Number concentration of particles	No./ cm^3
C_{mo1}	Operational and maintenance cost of flocculation	$\$/\text{yr}$	n_o	Influent concentration of particles	No./ cm^3
C_{mo2}	Operational and maintenance cost of sedimentation	$\$/\text{yr}$	R	Removal efficiency of sedimentation	-
C_{mo3}	Operational and maintenance cost of Filtration	$\$/\text{yr}$	t	Filtration time	min
C_{p1}	Capital cost of flocculation	$\$/\text{yr}$	t_f	Flocculation time	min
C_{p2}	Capital cost of sedimentation	$\$/\text{yr}$	UN	Number of sedimentation units	-
C_{p3}	Capital cost of filtration	$\$/\text{yr}$	V	Settling velocity	m/h
C_v	Fraction of particles having settling velocity equal or less than V	-	V_o	Filtration velocity	m/h
CCI	Construction cost index (divided by 100)	-	V_s	Overflow rate	m/h
d_c	Diameter of a filter grain	cm	α_1	Constant in flocculation model	-
d_f	Floc diameter	cm	α_2	Filter grain - particle attachment coefficient	-
d_p	Elementary particle diameter	cm	α	Particle - particle attachment coefficient	-
d_u	Ultimate floc diameter	cm	β	Fraction of particles retained on the filter grain which act as collectors	-
DHR	Direct hourly wage rate	$\$/\text{h}$	β'	Constant	-
F_r	Water content in the floc (in fraction)	-	μ	Absolute viscosity	$\text{g cm}^{-1}\text{s}^{-2}$
f	Filter porosity	-	ρ_s	Density of suspended particles	g/cm^3
G	Velocity gradient	s^{-1}	η	Contact efficiency of a single filter grain	-
h_f	Headloss	cm	η_p	Contact efficiency of a retained particle	-
k_2	Kozney's constant	-	η_R	Single collector removal efficiency	-

REFERENCES

- Boadway, J.D. (1978) Dynamics of Growth and Breakage of Alum Floc in Presence of Fluid Shear, *J. Env. Eng. Div., Proc. ASCE*, 104 (EE5) : 901-915
- Clark, R.M. (1982) Cost Estimation for Conventional Water Treatment, *J. Env. Eng. Div., Proc. ASCE*, 108 (EE5) : 819-834.
- Dick, R.I. (1982) Discussion on "Integral Analysis of Water Treatment Plant Performance", *J. Env. Eng. Div., Proc. ASCE*, 108 (EE2) :
- Liang, A.S. (1982) Technical Comparison of Direct Filtration and Contact Flocculation-Filtration, *Masters Thesis, Asian Institute of Technology, Bangkok, Thailand.*
- O'Melia, C.R. and Ali, W. (1978) The Role of Retained Particles in Deep Bed Filtration, *Prog. Water Techn.*, 10(5/6), 123-137.

SIMULATION OF EFFECTS OF GROUNDWATER
WITHDRAWAL ON CONSOLIDATION OF LAYERS

A. Das Gupta
Asian Institute of Technology
P.O. Box 2754, Bangkok, Thailand

J. Premchitt
Geotechnical Control Office
Public Works Department, Hong Kong

ABSTRACT

A generalized model coupling a quasi-three-dimensional hydrologic model with one-dimensional vertical consolidation model is presented for the simulation of effects of groundwater withdrawal on consolidation of layers in a multilayer groundwater basin. The hydrologic model was devised on the basis of the model introduced by BREDEHOEFT & PINDER (1970) with relevant modifications to suit the hydrogeological situation in the problem area. The actual stratification of the subsurface at selected locations in the model domain have been used in the simulation of consolidation. The model formulation with the emphasis on the adaptability of the model to a field situation having complex hydrogeological characteristics has been discussed. The subsurface is considered to be a single hydraulically connected body stratified into model layers for convenience in the simulation. Any number of model layers can be incorporated with coupling being provided through the leakage flux. The applicability of the model is demonstrated in the simulation of effects of groundwater withdrawal on consolidation of layers for the subsurface strata underlying the city of Bangkok, Thailand.

I INTRODUCTION

Land subsidence of great magnitude covering a large area has often resulted from the decline of piezometric pressure due to excessive water withdrawal from a multilayer groundwater basin. In the evaluation of subsidence due to deep well pumping, it is necessary to determine: (i) the drawdowns in the water bearing strata (sand and/or gravel layers) due to a time dependent pumping rate, (ii) the immediate compression of the strata due to these drawdowns, and (iii) the consolidation settlement of the clay layers under time dependent loading resulting from drawdowns in the adjacent water bearing strata.

The basic theories that describe the two phenomena involved in land subsidence due to groundwater withdrawal are those of THEIS (1935) and TERZAGHI (1925). Later, BIOT (1941) presented concise mathematical expressions that fully described the groundwater flow and stress-stress relationships in a soil in a three-dimensional domain, based on the theory of elasticity. SANDHU (1979) reviewed the development of land subsidence models and noted certain differences of opinion in setting up constitutive relationships. HELM (1982) compared major conceptual models of subsidence (depth-porosity, half-space, viscoelastic and elastic aquitard-drainage) and developed an alternative approach. In most of the situations, a one-dimensional deformation model is coupled with a two- or three-dimensional hydrologic model to calculate consolidation at selected points in the system. Full mathematical simulation of regional subsidence has been carried out for the case of Venice (GAMBOLATI & FREEZE, 1973; GAMBOLATI et al, 1974). The major limitation of this work is that the axis-symmetric hydrologic model used is an unrealistic representation of the actual situation. Various hydrologic model structures (PINDER & BREDEHOEFT, 1968; JAVANDEL & WITHERSPOON, 1969; BREDEHOEFT & PINDER, 1970; CHORLEY & FRIND, 1978; PREMCHITT, 1981) were devised for generalized and simplified situations with aquifers separated from each other by aquitards and extending conti-

nuously over the domain. In some cases, these assumptions may be oversimplified and it may lead to significant errors in the model simulation of real aquifer basin. Because of the variability of the sediments, delineation of aquifers and aquitards extending continuously over the domain from borehole data, especially for large areal extent multilayer groundwater basins created in fluvial or deltaic environments, is a difficult task, if not impossible, that often involves much speculation. It is desirable therefore to seek other approaches which do not employ the concept of aquifer but in which borehole data are fully utilized in the establishment of the model structure. The full three-dimensional model (FREEZE, 1971; GUPTA & TANJI, 1976; FRIND & VERGE, 1978) is flexible enough to handle this type of groundwater basin where the concepts of aquifer and aquitard are not applicable. Practical application of this model for the general cases of real groundwater basins is limited due to the non-availability of field data to characterize the system. Also there is serious computer limitations in terms of both time and storage to a full three-dimensional synthesis. In this context, the present paper emphasizes a simplified modeling approach for a multilayer groundwater basin with the objective of obtaining a practical model that combines the virtues of a sound theoretical basis, simple mathematical manipulation and computer programming and closely represents the real groundwater basin under consideration. The applicability of the model is demonstrated in the simulation of groundwater flow regime and associated consolidation for the groundwater basin underlying the city of Bangkok.

II GROUNDWATER SYSTEM IN BANGKOK, THAILAND

Bangkok is a city of 5 million people and more than one third of freshwater consumption in the metropolitan area is extracted from the water bearing strata underneath the city. These strata are a part of the large groundwater system of the Lower Central Plain of Thailand. Heavy utilization of groundwater began in the 1950's and the rate of extraction increased rapidly to the amount of more than $1 \times 10^6 \text{ m}^3/\text{d}$ in 1979. This exploitation is excessive and has caused drops in groundwater level at various depths from the original free flow artesian conditions (PIANCHAROEN & CHUAMTHAISONG, 1976) to more than 45 m below ground surface in 1979. Because of this excessive groundwater level drop, widespread land subsidence is taking place.

1. Basin Geology

The Lower Central Plain of Thailand was formed on geologic fault/flexure depression filled with clastic sediments. The subsurface strata overlying the basement were described as fluvial and deltaic sediments aged from Recent to Oligocene. The topmost stratum is called 'Bangkok Clay'. It is about 20 m thick in the Bangkok area and consists of about 12 m of soft marine clay stratum overlying 8 m of desiccated stiff clay stratum. In conventional definition the subsurface strata in the Bangkok area consist of eight aquifers existing to a depth of about 660 m (PIANCHAROEN & CHUAMTHAISONG, 1976) and these are named as follows: Bangkok aquifer (50-m zone), Phra Pradaeng aquifer (100-m zone), Nakhon Luang aquifer (150-m zone), Nonthaburi aquifer (200-m zone), Sam Khok aquifer

(300-m zone), Phaya Thai aquifer (350-m zone), Thonburi aquifer (450-m zone), and Pak Nam aquifer (550-m zone). These aquifers were defined according to the geological, hydrological and geophysical studies. Detailed interpretation of the compiled logs reveals that there exists great variation in subsurface strata and individual aquifer cannot be definitely differentiated, even in the small area of Bangkok (SODSEE, 1978), see Figure 1. Over the entire Lower Central Plain the complexities of the strata are much more pronounced, and there seems to be little lithological correlation between borehole logs.

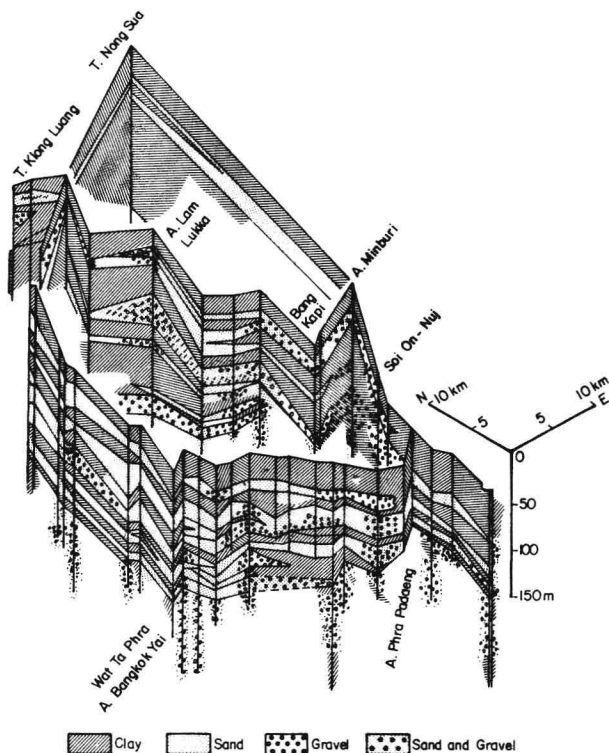


Figure 1 Fence Diagram showing Subsurface Strata in the Bangkok Area (after SODSEE, 1978)

Many clay strata are missing in some areas, while thickness of sand and/or gravel strata vary greatly from location to location. According to this interpretation, the concept of distinct separation between water bearing strata by continuous low permeability strata throughout the domain is untenable in this case. For this purpose, the groundwater system throughout the depth is considered as a single hydraulically connected body in schematizing the subsurface body for the mathematical model simulation. The random distribution of horizontal water bearing strata and the strata of very low permeability would create a subsurface body with very high permeability in the horizontal direction in comparison with that in the vertical direction. In this case, heavy groundwater pumping at a depth will cause a large drop in groundwater level at that depth with a low piezometric head gradient in the horizontal direction and a high piezometric head gradient in the vertical direction as shown hypothetically in Figure 2(a). While Figure 2(b) shows the actual vertical profiles of the groundwater level recorded from observation wells in the Bangkok area which indicate that there is vertical flow through alternate layers of sand and clay in addition to a much larger horizontal flow through the water bearing strata. With these results from field measurement it is more realistic to formulate the model structure on the basis of the actual hydraulic response and geologic stratification of the groundwater system and accordingly,

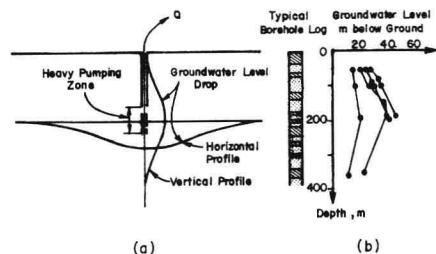


Figure 2 Typical Groundwater Level Profiles in a Multi-layer Basin. (a) Hypothetical Profile. (b) Vertical Profile from Field Measurement

model layers are defined.

III MATHEMATICAL FORMULATION

A quasi-three-dimensional hydrologic model coupled with one-dimensional vertical consolidation model has been used to simulate the effects of groundwater withdrawal on consolidation of various layers. The hydrologic model has been devised on the basis of the model introduced by BREDEHOEFT & PINDER (1970), but the proposed formulation by the said authors relied heavily on the concepts of aquifers with intervening aquitards extending continuously over the entire domain. Great effort in analysis and computation is required to include the effect of water released from storage in the aquitard (HERRERA & YATES, 1977; CHORLEY & FRIND, 1978; PREMCHITT, 1981). However, the continuous extension of the aquitard over the entire domain in the theoretical sense normally cannot be delineated in the actual large groundwater basin. Moreover it is realized that the effort in finding water released from the aquitard in a rigorous manner may not be worthwhile in the present case, since the subsurface configurations do not conform with theoretical assumptions. Therefore, even though the hydrologic model adopted in this case is based on the quasi-three-dimensional model structure, but the concepts and definitions of model parameters are different from those commonly employed.

1. Hydrologic Model

According to quasi-three-dimensional model structure in the finite difference formulation, the unit element is a block with horizontal area $\Delta x \Delta y$ and with thickness ℓ . For the present formulation the unit element contains the water bearing stratum as well as the random distribution of clay layers of very low permeability, as illustrated in Figure 3. The governing equation for groundwater flow for this unit volume can be derived from continuity concept and expressed as

$$\frac{\partial}{\partial x} K_x \ell \frac{\partial h}{\partial x} + \frac{\partial}{\partial y} K_y \ell \frac{\partial h}{\partial y} = S' \frac{\partial h}{\partial t} + Q + \frac{K_z \ell}{\ell} (h - h_u) + \frac{K_z \ell}{\ell} (h - h_l) \quad (1)$$

where, K_x and K_y are the principal permeability vectors coinciding with the cartesian coordinate directions; h is the hydraulic head of groundwater; S' is the coefficient representing storage behavior of the system; Q stands for the groundwater extraction term; and the last two terms on the right hand side represent the leakage flux between the adjoining layers and the layer under consideration. Since the adopted unit element also contains very low permeability clay layers instead of unit element of aquifer as has been commonly employed, the definitions and concepts of the parameters are different. The following discussion provides definition of each term appearing in Equation 1 in order to clarify these differences.

The terms $K_x \ell$ and $K_y \ell$ are the product of average horizontal permeability and the unit element thickness. These terms are used in place of the commonly used transmissivity, T , which is the horizontal permeability of the aquifer multiplied by the aquifer thickness. With the assumption that all water bearing strata (sand and/or gravel layers) within a given thickness ℓ have almost the

same value of permeability, represented by K , and the permeability of all clay strata within a given thickness ℓ be represented by K_c , then the terms $K_x \ell$ (and $K_y \ell$) can be found as follows

$$K_x \ell = K_s \sum b_s + K_c \sum b_c \quad (2)$$

where b_s and b_c are the thickness of the individual sand and clay layers at a particular location and depth; and $\sum b_s + \sum b_c = \ell$. For practical purposes $K_x \ell$ (and $K_y \ell$) can simply be approximated by $K_s \ell b_s$, since K_c is much smaller than K_s .

The hydraulic head h is the head in the layer under consideration and it represents the head at the centre of the unit element shown in Figure 3. The heads h_u and h_l are the heads in the upper and lower model layers respectively and they represent the heads at the centres of the adjacent layers. In the conventional definition the head h is assumed to be the same over the thickness of the aquifer. For this formulation the head h represents only the head at the centre of the unit element, and a straight-line variation is assumed for the head between the centers of two adjacent unit elements in the vertical direction.

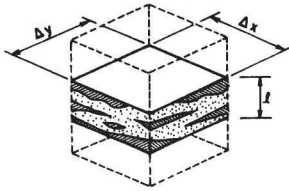


Figure 3 Unit Element in the Analysis of Flow in a Multi-layer Ground-water Basin

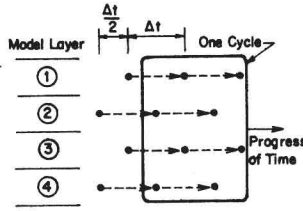


Figure 4 Staggering of the Time Step in Alternate Model Layers

The terms K_{zu}/ℓ and K_{zl}/ℓ are called seepage factor and their magnitudes control the flow from the layer under consideration to the upper layer and lower layer, respectively. K_{zu}/ℓ (and K_{zl}/ℓ) can be expressed in terms of K_c and K_s (adopted for vertical permeability in this case) as follows

$$\frac{K_{zu}}{\ell} = \left(\frac{\sum b_s}{K_s} + \frac{\sum b_c}{K_c} \right)^{-1} \quad (3)$$

In the same way as the horizontal permeability the seepage factor can be approximated by $K_c/\ell b_c$ at a particular location and depth. The characteristics of the layered system with high permeability contrast are such that the vertical permeability is dependent on the low permeability clay strata even where the cumulative thickness of the clay layers is only 5-10% of the model layer thickness, while the horizontal permeability is dependent on the high permeability sand strata in the same manner. Therefore the K_s to be used in the expression $K_s \sum b_s$ should be the horizontal permeability of the sand layer and the K_c to be used in $K_c/\ell b_c$ should be the vertical permeability of the clay layer.

The parameter S' , unlike the storage coefficient S of an aquifer, includes the storage in the sand layers as well as the high storage in the clay layers existing in the model layer. The release of water stored in clay layers is delayed and the delay time depends on permeability, specific storage, and the thickness of the clay layer, according to Terzaghi's theory of consolidation (TERZAGHI, 1925). Application of the theoretical analysis of these delay effects for the cases of aquifers separated throughout the domain by aquitards to the simulation of an extensive groundwater system seems to be of insignificant value because of the complexities of the subsurface forma-

tion and random distribution of aquitard. Therefore the parameter S' defined here simply includes both the storages of the clay and sand layers as

$$S' = S_{ss} \sum b_s + S_{sc} \sum b_c \quad (4)$$

where S_{ss} is the specific storage of sand layers and S_{sc} is specific storage of clay layers in a model layer. Generally, S_{sc} is much higher than S_{ss} , and therefore S' can be approximated as $S_{sc} \sum b_c$. The value of S' is invariably higher than the value of S commonly obtained from a pumping test in a coarse grained stratum.

2. Consolidation Model

The consolidation model is developed to find (i) the piezometric head distribution in clay layer, and (ii) the magnitude of the compression of each slice, Δz of the clay layer and to sum these to represent the layer compression. The governing equation for the piezometric head in a clay layer assuming vertical flow is

$$\frac{\partial}{\partial z} K_z \frac{\partial h_c}{\partial z} = S_{sv} \frac{\partial h_c}{\partial t} \quad (5)$$

which is equivalent to

$$\frac{\partial}{\partial z} c_v \frac{\partial h_c}{\partial z} = \frac{\partial h_c}{\partial t} \quad (6)$$

where h_c is the piezometric head in the clay layer; S_{sv} is the specific storage of clay layer; and $c_v = K_z/S_{sv}$ is the coefficient of consolidation. The compression of each slice, Δz , caused by the piezometric head drop $-\Delta h_c$ is found from the void ratio (e) versus logarithmic of effective stress (\bar{p}) relationship by the following procedure.

The change in the void ratio, Δe , at the time t_n , due to the head change $-\Delta h_{cn}$ is calculated from

$$\Delta e_n = C \log \left(1 - \frac{\Delta h_{cn} \gamma_w}{\bar{p}_{n-1}} \right) \quad (7)$$

$$\Delta h_{cn} = h_{cn} - h_{cn-1} \quad (8)$$

where the subscript c indicates a clay layer, n indicates the number of time step, and γ_w is the unit weight of water. The magnitude of the compression for each slice of thickness Δz is given by

$$\Delta \rho_n = \frac{\Delta e_n}{1 + e_{n-1}} \Delta z \quad (9)$$

and the magnitude of the clay layer compression is found from

$$\rho_{cn} = \rho_{cn-1} + \sum \Delta \rho_n \quad (10)$$

The value of \bar{p} and e are then changed to be the initial values for the next time step, thus

$$\bar{p}_n = \bar{p}_{n-1} - \Delta h_{cn} \gamma_w \quad (11)$$

$$e_n = e_{n-1} - \Delta e_n \quad (12)$$

If the maximum effective stress that the slice Δz has ever experienced is p_m , C takes the value of the compression index, C_c , when (i) $\bar{p}_{n-1} = p_m$, and (ii) Δh_{cn} is negative. If one of these two conditions is not satisfied, C takes the value of the swelling index, C_s . The magnitude of the compression of model layer of high permeability is found from

$$\rho_{an} = S' \Delta h_n \quad (13)$$

where S' can be employed to represent the compressibility of model layer. Finally, the subsidence at a point on the ground surface is the summation of the compression of all the soil layers beneath that point and is given by

$$\rho_{tn} = \sum (\rho_{cn} + \rho_{an}) \quad (14)$$

It should be noted that almost all previous workers on the prediction and simulation of land subsidence based their calculation on a linear stress-strain relationship. The use of the true e - $\log \bar{p}$ relationship for the clay is obviously a better basis for the prediction of subsidence. From rigorous analysis, the use of e - $\log \bar{p}$ relationship to

represent the clay compressibility in the estimation of clay layer compression is not compatible with the consolidation equation (Equation 5) in which S_{sv} and K_z are independent with respect to stress and time. The linear relationship between e and $\log \bar{p}$ implies that the compressibility of clay is dependent on the applied stress \bar{p} . In this case S_{sv} may be expressed as

$$S_{sv} = \frac{0.435 C_{\gamma_w}}{(1+e_o) \bar{p}_{av}} \quad (15)$$

where \bar{p}_{av} is the average stress.

3. Numerical Approach

The detailed technique for solving the system of equations in an alternating direction implicit finite difference formulation of Equation (1) for a model layer can be found elsewhere (PEACEMAN & RACHFORD, 1955; PINDER & BREDEHOEFT, 1968; RUSHTON, 1974). The technique is extended to be applicable to a multilayer problem. In solving for the piezometric head in a particular model layer, there are two other unknown terms, the piezometric heads in the upper and lower model layers (h_u, h_l) appearing in the leakage flux terms. Solving these equations directly is approximately equivalent to solving the full three-dimensional model, which will need much more computing effort. To avoid this, a time lag of $\Delta t/2$ (half time step) between the progress of time in any two adjacent model layers has been used in the solution process, as demonstrated in Figure 4. While evaluating the head for a particular model layer from the time t to $t + \Delta t$, the heads in the two adjacent model layers are the known values at the time $t + \Delta t/2$, and they are assumed to be constant over the period. With the calculated value of head in this model layer at time $t + \Delta t$, the solutions in the two adjacent layers are then evaluated from time $t + \Delta t/2$ to $t + 3\Delta t/2$. In this process, the odd-numbered model layer (layer 1, 3, ...) are solved simultaneously, and the time progressed from t to $t + \Delta t$. Then the even-numbered model layers (layer 2, 4, ...) are solved, and the time progressed from $t + \Delta t/2$ to $t + 3\Delta t/2$. With the completion of this cycle of calculation the time increases by one time step, Δt , for all model layers, but the head in each model layer corresponds to a time lag of $\Delta t/2$ from the two adjacent model layers.

The piezometric head in the model layers derived from the hydrologic model are used as the boundary piezometric heads for the consolidation model (Equation 5) for an individual clay layer at any location. The Crank-Nicholson scheme has been employed to formulate the finite difference equations for the consolidation model.

IV APPLICATION OF THE MODEL

In order to make a realistic estimation of the future response of the groundwater system, proper representation of the actual system characteristics in the model is necessary and the model behavior should agree closely with the real responses of the groundwater system. The model simulation was carried out in three stages, namely, (i) preparation of the model structure and specification of system characteristics on the basis of the available information and results from laboratory and field tests, (ii) model calibration, in which various parameters are adjusted in trial computer runs to achieve model results which represent the actual performances observed from field measurement and (iii) prediction of future response under various possible groundwater pumping schemes. The first stage has been dealt in detail in an earlier paper by PREMCHITT & DAS GUPTA (1981). Also calibration of the hydrologic model and results of sample prediction runs were presented in that paper. Only salient features in discretization, simulation for land subsidence are covered in this section.

Most of the groundwater extraction in Bangkok area is from the 100 - to 200 - m depth zone and the pumping effects are small in a very deep zone. Therefore, on the basis of field measurement of hydraulic head variation with depth, the model was established to a depth of 400 m,

including all strata that have significant influence on basin responses. The available pumping tests and hydraulic head measurements in Bangkok have been conducted according to the conventional definition of aquifers. In order to utilize the results from these tests and measurements fully, the total thickness of the subsurface body considered has been divided into six model layers corresponding to the six conventional aquifers. Areal boundaries of the model have been specified on the basis of the following criteria: (i) distribution of relative abundance of water bearing strata, $\Sigma b_s/l$, (ii) distribution of specific capacity, (iii) configuration of bed rock, and (iv) geological interpretation. The selected model boundary encompasses the region of high specific capacity and the area where relative abundance of water bearing strata is greater than 30%.

1. Model Calibration

In the Bangkok area, appreciable groundwater pumping began in the 1950's, and field information on groundwater levels become available since that time. The trial model simulation to calibrate various model parameters has therefore been conducted for the time period 1955-1979. Insignificant groundwater extraction has taken place prior to 1955, and it is reasonable to assume the initial condition in 1955 to be in steady state condition over the domain. The groundwater flow domain has been discretized into blocks of unit element, the sizes of which are 5 km by 5 km, and model thicknesses are 50 m for layers II, III and IV, 75 m for layers I and V, and 100 m for layer VI. A uniform time step of 3 months has been employed in the simulation.

During the calibration process, several trial simulations are carried out while the model parameters are adjusted within the stipulated ranges until the model results agree satisfactorily with the field observations. In the simulation for land subsidence, emphasis has been placed to achieve the pattern and magnitude of subsidence in 1978-79, in which re-leveling of the existing benchmarks has been carried out for the first time since they were installed in 1930's. The results from these trial simulation are presented in Figures 5 and 6. In Figure 5, the variations of groundwater pressure with depth in the clay and sand strata derived from model simulation are compared with the field measurement of 1979. The profile of surface subsidence in Figure 6 along section AA' which passes through most of the existing benchmarks has been considered in the simulation and the simulated results agree reasonably well with the field measurement. Typical characteristics of the calibrated hydrologic model are given in Table 1 comparing with the ranges of values estimated from field and laboratory tests. While typical calibrated values of the coefficient of consolidation for clay layers, c_v , in comparison with laboratory test results are given in Table 2. These values result in the distributions of pore water pressure in the clay layers approximately equal to those observed in the field. The values of compressibility parameter, C_c , used in the model are given in Table 3 and compared with the estimates from field measurements and from laboratory tests.

Table 1 Hydrologic Parameters Estimated From Test Results Using $\Sigma b_s/l = 0.6$ in Comparison with Model Parameters (Layer III) in Bangkok Area

Parameter	Range of Value from Test Results	Model Value
$K_h l \sim K_s \Sigma b_s$	1500 - 3600	3325 m ² /d
$K_v/l \sim K_c/\Sigma b_c$	2.5 - 25 x 10 ⁻⁶	16 x 10 ⁻⁶ d ⁻¹
$S' \sim S_{sc} \Sigma b_c$	1.0 - 4.0 x 10 ⁻³	1.0 x 10 ⁻³

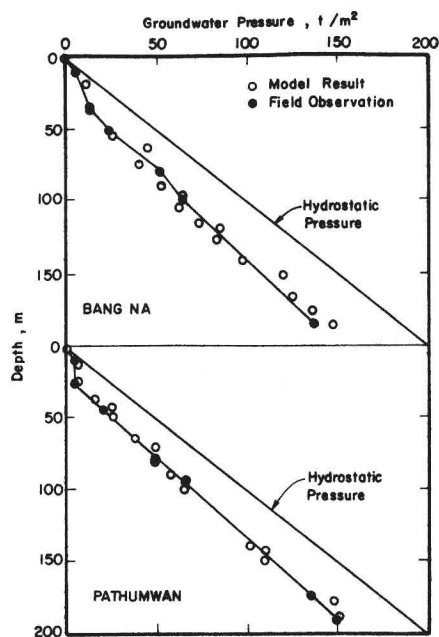


Figure 5 Variation of Groundwater Pressure with Depth at Two Subsidence Model Stations in 1979

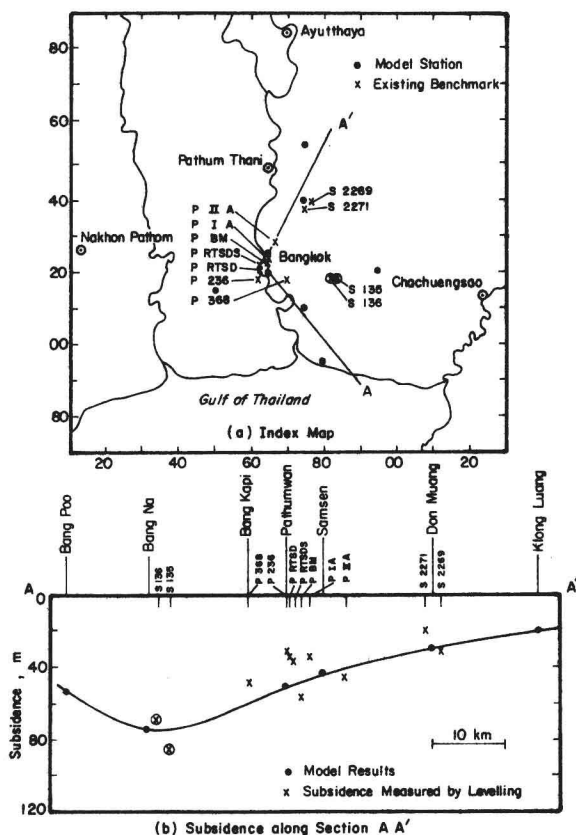


Figure 6 Model Results in Comparison with Field Measurement for Land Subsidence in Bangkok in 1979

Table 2 Typical Calibrated Parameter c_v for Clay Layers in Comparison to Laboratory Test Results

Type of Clay Layer	$c_v, 10^{-4} \text{ cm}^2/\text{s}$	
	Model Value	Laboratory Test Results
Soft Clay	1.2 - 3.4	1 - 5
Stiff Clay	12 - 24	1 - 10
Hard Clay	17	1 - 10

Table 3 Model Compressibility in Trial Simulation in Comparison with Other Estimates

Type of Clay Layer	C_c Model	C_c Estimated from Field Measurement, 1978-79	C_c Laboratory Test Results
Soft Clay	0.25	0.05	0.2 - 0.5
Stiff Clay	0.03	0.015	0.04 - 0.15
Hard Clay	0.03	0.03	0.02 - 0.10
Sand	0.003		0.01 - 0.04

2. Model Prediction

The objective is to focus attention on the alarming possibility of the future general subsidence of Bangkok as a result of the extensive deep well pumping now underway in the area and also to give a general idea on how effective will be the control measures on pumpage to slow down the subsidence. In one scheme (Scheme A), 5% annual rate of increase in groundwater pumpage is assumed for the next twenty years starting from the year 1979 as the basis. This scheme represents more or less the present pattern of increase in pumpage. Another hypothetical scheme of controlled pumpage is considered to evaluate its effectiveness in reducing the rate of subsidence. This scheme (Scheme B) stipulates that the control becomes effective immediately from the year 1980 and the total pumpage is maintained more or less constant up to the year 1985 with a slight reduction by that time. After 1985, the pumping rate is reduced to the amount of 750,000 m^3/d and this rate is maintained constant up to year 2000. Pumping centers in the model configuration are assumed to be same for the two schemes and increase and decrease of pumpage are in the same proportion as in 1979. With an annual increase in the pumpage at the rate of 5%, the groundwater level will drop more than 90 m below the ground surface in model layer III and the surface subsidence will be more than 2 m by 2000 as shown in Figure 7. However by controlling the total pumping rate to be 750,000 m^3/d after 1985, the model predicts recovery of groundwater level to about 25 m below the ground surface with subsidence of slightly more than 1 m by 2000. These results indicate that with substantial reduction in pumpage the progress of subsidence will be much slower than with the uncontrolled situation.

The model described here consists of about 4000 blocks of unit element. The computer storage required is 300×10^3 bytes. Execution time for a period of simulation of 25 years or 100 time steps is 15 min (0.15 min per time step) on the IBM 370/145 computer. The equivalent full three-dimensional model with the same number of unit elements would require a complex solution scheme for the three-dimensional structure of the elements (FREEZE, 1971; GUPTA & TANJI, 1976), and the other quasi-three-dimensional model would require the addition of more than 10 times the number of elements in the aquifer models to represent aquitards (CHORLEY & FRIND, 1978; PREMCHITT, 1981).

V CONCLUSION

A generalized model coupling a quasi-three-dimensional hydrologic model with one-dimensional vertical consolidation model is presented for the simulation of effects of groundwater withdrawal on consolidation of layers in a multilayer groundwater basin. The model is formulated as